MICROSTIMULATORS AND MICROTRANSDUCERS FOR FUNCTIONAL NEUROMUSCULAR STIMULATION

Contract #N01-NS-5-2325
Quarterly Progress Report #13
Period: March 10, 1998 - June 9, 1998

ALFRED E. MANN FOUNDATION FOR SCIENTIFIC RESEARCH
12744 San Fernando Road, Sylmar, CA 91342
Joseph H. Schulman, Ph.D., Principal Investigator
John Gord

BIO-MEDICAL ENGINEERING UNIT, QUEEN'S UNIVERSITY
Kingston, ON K7L 3N6 CANADA
Frances J.R. Richmond, Ph.D., Principal Investigator
Gerald Loeb, Kevin Hood, Ray Peck, Anne Dupont, Tiina Liinamaa

PRITZKER INSTITUTE OF MEDICAL ENGINEERING, ILLINOIS INSTITUTE OF TECHNOLOGY
Philip R. Troyk, Ph.D., Principal Investigator

Abstract

We are developing a new class of implantable electronic devices for a wide range of neural prosthetic applications. Each implant consists of a microminiature capsule that can be injected into any desired location through a 12 gauge hypodermic needle. Multiple implants receive power and digitally-encoded command signals from an RF field established by a single external coil. The first two types of implant that we have made were single-channel microstimulators equipped with either a capacitor-electrode or an internal capacitor that stores charge electrolytically and releases it upon command as current-regulated stimulation pulses. We are also working on implants equipped with bidirectional telemetry that can be used to record sensory feedback or motor command signals and transmit them to the external control system.

Work at Queen's concentrated on revisions and testing of the glass package using equipment, fixtures and parts transferred from AEMF, which is concentrating on package hermeticity and the stimulation circuit. High yields of hermetic seals and complete, working BIONs were obtained using glass-to-tantalum techniques at both ends of the capsule; chronic testing is underway.

Work at Queen's University has concentrated on revision and qualification of the various hermetic, electrical and mechanical seals involved in the glass package, while work on the package hermeticity and stimulation circuit continues at AEMF. A glass packaging system was shipped to and installed at Queen's under the supervision of Gerald Loeb and Ray Peck. In particular, a CO_2 laser used for all glass-to-metal and glass-to-glass seals with reconfiguration to improve beam focus and alignment and new collets were included in the Queen's equipment. Metal-to-metal seals were made previously on the production YAG laser at Advanced Bionics Corp.; no similar facility exists at Queen's. Initial attempts to use the infrared CO_2 beam in place of the ultraviolet YAG beam were unsuccessful because of inability to control the amount of light reflected from the metal surfaces. Pilot experiments in the Queen's Physics Dept. indicated that a plasma needle arc welder could be used successfully, so one was purchased and installed in the BION microfabrication facility at Queen's.

The various seals are numbered in the attached Assembly Tree shown on page 8 and their fabrication techniques and results are discussed in order below:

#1.-2. PtIr washer to Ta electrode stem

This is a mechanical and electrical connection that is entirely inside the package. It provides a noble metal contact between the Ta stimulating electrode and the gold-plated butt end of the μPCB. The weld is done after the glass washer is threaded onto but not yet melted onto the Ta stem, so there is no danger of damaging a hermetic seal. We use the plasma needle to melt a small ball onto the end of the Ta stem and then resistance weld the ball to the inside edge of the hole in the PtIr washer. All of the completed BIONs described in this report were made in this manner. The disadvantage of this

technique is that there is occasionally some splatter of the Ta ball material onto the PtIr face, which might interfere with reliable electrical contact if it comes between the washer and the gold μPCB contact. Subsequent experience with a similar weld to the Ir electrode (see below) indicates that the connection of the stem to the PtIr washer can be made with the plasma arc, either as a continuation of the ball-making process or as a second pulse of energy after repositioning the washer against the back of the just-formed ball. This greatly accelerates production but it requires a more complex fixture that we are now building to test this concept.

#3. Glass bead to Ta stem

The CO_2 laser beam melts the glass onto the Ta stem as the parts rotate in the beam path. This seal has been extremely reliable ever since we started specifying a particular Ta wire material and surface finish for use as stems in the manufacture of the sintered Ta slugs. There was no problem in reproducing this seal with high reliability at Queen's.

#4. Glass bead to glass capillary to form capsule subassembly

The CO_2 laser beam melts the end of a precut glass capillary tube to the outside edge of the glass bead that has been melted onto the Ta stem, forming an open-ended capsule as shown in the insert figure at the bottom of the left branch of the Assembly Tree. At that stage, the Ta electrode feedthrough can be tested for hermeticity under optimally sensitive conditions (2×10^{-11} cc atm He/s) and for residual stress in the glass using photoelastic polarimetry. This seal has also been reliably hermetic, but there have been some difficulties in the past in obtaining the desired mechanical shape and low,

compressive stress levels. The improved mechanical jigging and laser beam control solved these problems.

#5. Glass bead to Ta tube feedthrough

This has been the most problematic weld for the past year. As described in previous progress reports, we abandoned the use of PtIr tubing because incompatibility with the thermal coefficient of the glass caused a high rate of delayed failures of the seal after a few weeks of soaking and temperature cycling in saline. We demonstrated last fall that Ta could be used electrochemically in conjunction with the Ir electrode under conditions of chronic charging and stimulation without corrosion of any metals. However, many attempts to use various batches of Ta tubes to make glass seals all had unreliable hermeticity. After extended discussions with vendors and consultants and several key experiments, we arrived at an understanding of and solution for the problem.

The Ta material that must be used to draw tubes (as opposed to wires) is slightly different in trace chemical composition from that used for the stem wires, but that turned out to be a red herring. More importantly, the tube material must be vacuum annealed at various stages during the drawing process to remove adsorbed gasses, particularly oxygen, that change its handling properties. We had neglected to request the suppliers to conduct a final vacuum anneal on the fully drawn tubes. When we annealed existing tube lots, the relatively smooth surface texture immediately lit up with longitudinally oriented oxide trails, presumably related to oxygen leaching to the surface at crystal grain boundaries. The vacuum annealed surface is now abraded down to bare metal by 24h tumbling in abrasive media, which leaves a grainy but amorphous surface and eliminates longitudinal draw marks, which were quite prominent in some tube lots. The end of the

tube where the glass bead is to be sealed is then rotary polished using diamond paste on a high speed wheel buffing, leaving a mirror-like surface. The CO2 laser is used to melt a glass bead onto the tube in a manner similar to the bead-to-Ta stem seal, with similarly reliable, hermetic, low-stress results. Half-capsules with these materials and processes have been soaked for a week in saline without loss of hermeticity. Long-term soak testing is underway.

All existing stocks of variously dimensioned Ta tubes appear to seal reliably to the borosilicate glass when treated in the proscribed manner. We have repeatedly replicated the problems of slow leaks when any of these tubes are sealed from stock that has not been vacuum annealed or from vacuum annealed stock that has not been adequately polished. We have settled on the thinner wall tube (0.012" i.d. x 0.020" o.d.) because it minimizes the longitudinal transmission of heat when the end of the tube is melted shut, which can crack the glass bead.

#6. Elgiloy spring to Ta tube

In the previous design, the inside end of the tubular feedthrough was welded to a PtIr washer. As the finished capsule was closed, this washer was compressed against a loose spring that in turn made mechanical and electrical contact with a gold-plated socket in the end of the μPCB. In the revised design, we have eliminated the PtIr washer and handling problems associated with the loose spring by resistance welding the end of the spring directly onto the end of the Ta tube as it projects through the glass bead. This is a simple and reliable cross-weld that must sustain only about 40g shear force from spring compression in the package. However, the weld and adjacent spring turns can be subjected to high temperatures during the glass-to-glass seal of the capsule closure step

(#8., see below), which risks oxidizing the gold-plating and losing the spring temper. Improved fixturing and control of the laser beam eliminated this problem even when the spring was welded to the Ta tube within 0.5 mm of the glass bead.

#7. Solder termination of Cu coil windings to μPCB - part of electronic subassembly

This connection will be discussed in the next quarterly report.

#8. Closure of glass capsule subassembly to glass bead on tubular feedthrough

This glass-to-glass seal is similar to #4 with the additional consideration that the parts must be rotated while being held under compression for the spring. The end of the tube must be kept unobstructed to allow expanding gas to escape. Also, the glass capsule subassembly may not be perfectly cylindrical because of melting to form the Ta electrode feedthrough. These factors pose some additional complications for the design of the collets used to hold the parts during the seal, but these have been overcome, resulting in high yields of capsule profiles that are hermetic, mechanically smooth, robust, symmetrical and cosmetically attractive.

#9.-10. Final seal of tubular feedthrough and attachment of Ir electrode

As is done with many hermetic implants, the final seal is the melting shut of a small all-metal port after vacuum bake-out and back-fill of the capsule with inert gas. This supposedly simple seal had proven difficult to achieve reliably with the YAG laser. Some problems were related to the formation of brittle alloys between the Ta tube and the adjacent Ir electrode or a Pt filler wire used to braze the tube shut. Others were related to heat pulse conduction down the tube to the nearby glass bead. The attachment of the Ir washer (which acts as the anodal stimulus electrode) to the side of the thin-walled Ta

tubing had also proven to be difficult, with inconsistent mechanical strength and occasional melt-through and cracks in the tube walls.

In the present strategy, we use the plasma needle arc to melt the end of the Ta tube into a small ball of pure Ta. The Ir washer is strung onto the tube before the ball is formed and then shifted against the back side of the ball after it is formed. A second brief arc heats the Ta ball to the melting point of the Ir washer, which fuses to the Ta where it makes contact. Both welds can be made reliably provided that there is about 1 mm of free tube length from the melted ball to the glass in order to accommodate heatsinking and ground connection to the tube. We are still refining the fixturing to see if we can further reduce this projection and to identify the effects of different Ir washer thicknesses. We also need to work out parts handling techniques to assure retention of the inert atmosphere in the capsule during sealing.

BION™ Glass Package Assembly Tree:

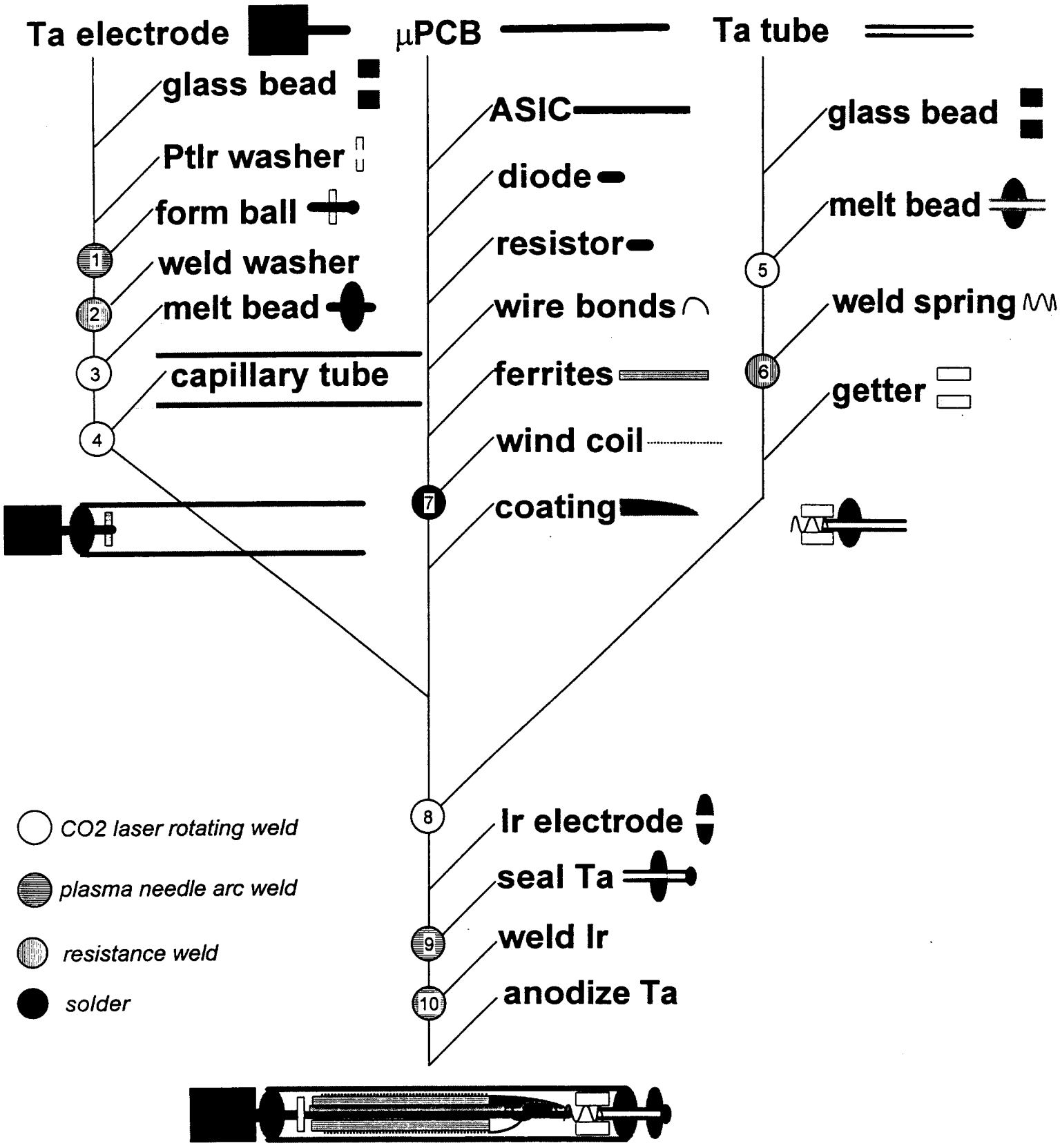

Glass-Encapsulated BIONs

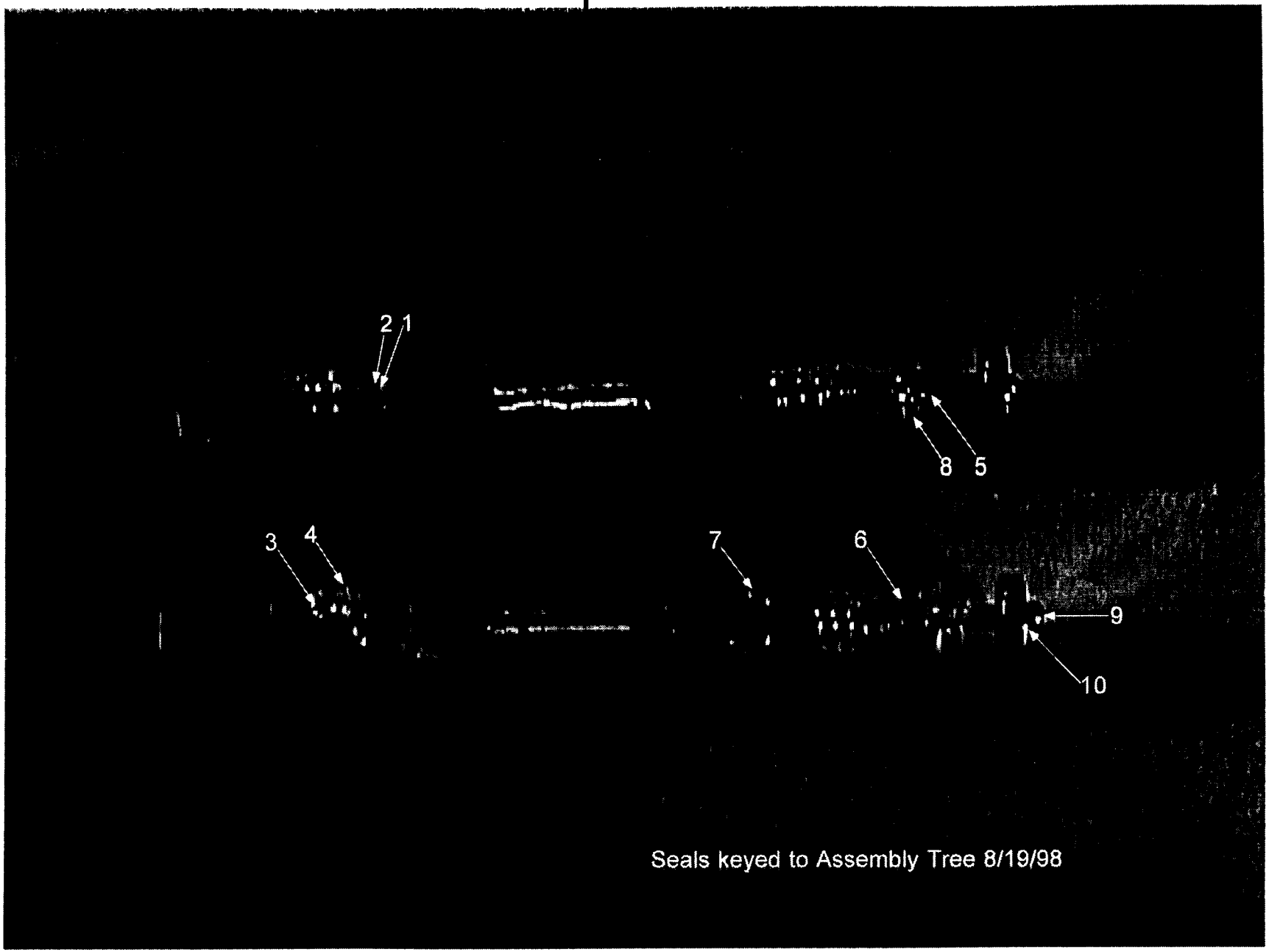

Qualification Testing

A full set of 8 working BIONs (using the original ASIC and epoxy μPCB and a tapered spring) have been assembled (see attached photograph) and started on chronic, active saline soak and temperature cycle testing (continuous maximal rated output, 3h @37 C & 9h @77 C). Another group has been sent to AEMF for high pressure bomb and bubble testing of the hermetic seals. Results will be reported next quarter. All of these units were vacuum baked at 90C for 24 hours and back-filled with the plasma arc shield gas (70% Ar, 25% He, 5% H). No getter was incorporated into the package.

The glass package design is fully compatible with the latest revision of the new μPCB and with the new ASIC, which involves a polarity reversal of the electronic subassembly. A small stock of the slightly shorter glass capillary tubes and the straight (untapered) springs required for this subassembly are already on hand. The anodization equipment will produce the 70V compliance voltage required to achieve 4X overvoltage anodization for use with the projected 17VDC electrode charging voltage. Techniques have been developed previously to produce the cylindrical getter that goes over the spring, but new molds will need to be machined. We anticipate conducting all accelerated life-testing without getter to increase sensitivity to any retained or incoming moisture. We will also supply IIT with a small number of sealed packages with the moisture sensing substrate for their soak testing and impedance spectroscopy.

IMPROVED 2-MHZ MICROSTIMULATOR ASIC DEVELOPED AT AEMF

Yield Problems Resolved

Work at the Mann Foundation concentrated on yield problems. As indicated in the last report, yield of microstimulators after attachment of the ferrite cores was poor -- but previous units had been assembled in a very similar manner with good yield. Tests were run in which the ferrites were glued in place, but the glue was not cured. After stripping the uncured glue, new surface scratches on the chips were observed, indicating that the ferrite placement actually gouged the chip surface. Why did this not show up before? The reason has to do with additional processing which was done on the earlier chips. The microstimulator design originally called for a chip mounted on a ferrite shelf, with the top of the chip uncovered (and hence not scratched by the ferrite). The design was revised to place ferrite core halves under and over the chip. To accommodate this, the pad locations on the chip had to be rearranged to put all the pads at one end of the chip. Existing chips were modified by adding another metal layer to route the exiting pads to the new pad locations. Before this additional metal layer was put down, a relatively thick protective layer was first placed over the whole chip to act as an inter layer dielectric. It was this thick protective layer which protected the earlier chips from damage by the placement of the ferrites. We will include such a protective layer in the next run of chips.

Another yield issue which was resolved during the quarter was related to coil tuning. The coil resonant frequency is monitored during winding and turns are added until a target frequency is reached. The target frequency is slightly high, since connecting the coil to the rectifier drops the frequency a bit due to rectifier and substrate capacitance. The assumption is that the frequency drop will be consistent unit to unit -- but testing after attaching the coil lead to the substrate showed a considerable range of shifts. The problem was finally traced to a solvent cleaner: after the coil lead is attached, the

substrate is cleaned. Some of the cleaning solvent is absorbed by the insulation of the coil wire, causing a frequency shift which depends on how long the assembly is allowed to dry. Consistent results were finally obtained by performing a short bake-out before testing the frequency.

Pulse Width Consistency

Testing of microstimulators under marginal signal conditions revealed a problem which has been present for years but which had gone mostly unnoticed: pulse width variation with weak signals. When such variations had been seen in the past, they were assumed to be due to double-bit errors in the received data (double bit errors are not detected by parity check). In recent testing, however, pulses with width errors were seen, but there were no missing pulses. (Missing pulses would indicate single bit errors.) It seemed unlikely that weak signals could produce many double bit errors without producing any single bit errors.

Further investigation showed that the problem could not be explained by ordinary bit errors at all: pulses were being produced which could be wider than the maximum design width. The problem was finally traced to the reset circuitry for the counter. To save space, a single 8-bit counter is used for several purposes. It keeps track of bits within a frame, it times pulse widths, and it times the delay after a pulse before a new one can be initiated. Because of these multiple uses, it also has multiple reset sources. During the normal decoding of incoming data frames, the counter is reset whenever an invalid bit is received (a zero where the frame format specifies a mandatory one, for example). Unfortunately, this reset path remained active after the start of an output pulse. As a result, the counter would be held reset until a "zero" bit was received after the start of the output pulse. Normally, there is a zero received right away, but in marginal signal conditions the sudden change in chip current consumption caused by the start of output pulse generation can cause data errors immediately after the pulse starts. If one or more

errors occur at that time, the counter is held reset and the pulse width is extended by the time that elapses before a "zero" is received.

Once the source of the problem was located, the fix was simple: disable the errant reset path once the stimulus pulse has started. This change will be made in the next run of chips.

BIDIRECTIONAL TELEMETRY AND 470 kHz CIRCUITRY DEVELOPMENT AT PRITZKER

During the last quarter work at the Pritzker Institute has focussed on analysis of MOS7 and refinement of the bi-directional rectifier and telemetry system.

In a previous report we described our difficulties in eliminating the parasitic bipolar transistors which produced a drain on the power supply when the lower rectification elements conducted into the substrate. MOS7 used a new guard band structure and synchronous rectification on the lower bridge elements to avoid this problem. In addition we included a local oscillator to test the reverse telemetry. A layout of MOS7 appears below with sections of the circuit identified.

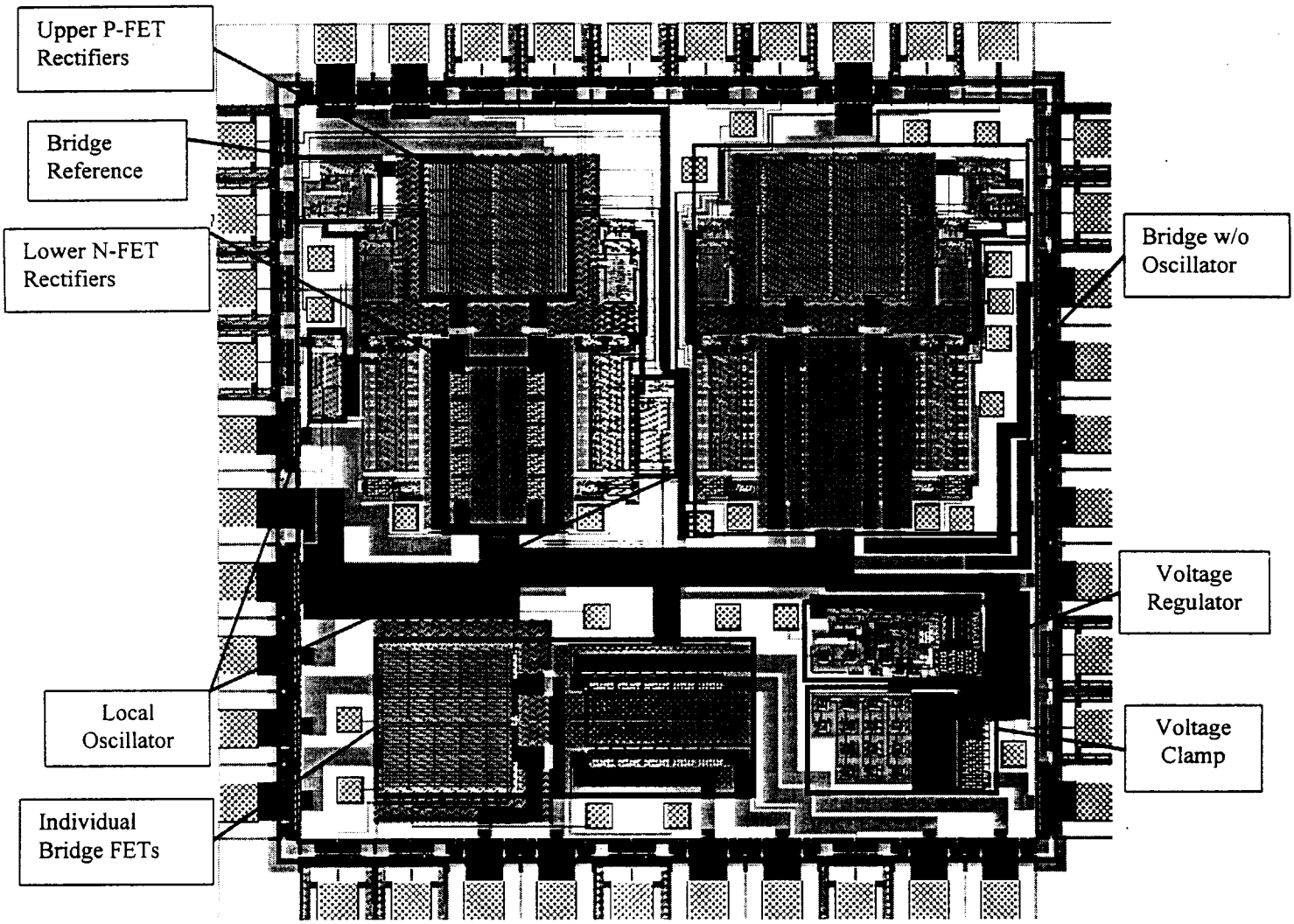

Included on MOS7 were two bridge designs, one with an oscillator and one without, individualized bridge FETs, a voltage regulator, and a voltage clamp. Around the

rectifying transistors used in the bridges, the guard ring structure described in our last QPR was used.

We evaluated the effectiveness of our strategy to eliminate the parasitic bipolar action by performing a series of curve tracer measurements upon the MOS7 bridge circuits. We were clearly able to see the combined effects of the synchronous rectification as well as the guard bands. When we disabled the drive to the lower N-FETs, the horizontal bipolar transistors turned on and pulled excessive current from the power supply. With the drive activated, the forward drop on the N-FET was significantly less than that required to forward bias the base-emitter junction of the bipolar. Therefore there was no parasitic current pulled from the power supply. With this success, we have contemplated variations on this structure to reduce the size of the rectifier transistors, as well as change the type to all N-FETs. Using N-FETs for the lower and UPPER rectifiers will eliminate the need for the floating N-Well of the upper P-FET transistors. This in turn will eliminate the need for the extensive guard band structure. We have already fabricated an all N-FET bridge, as part of another program, and we will be evaluating its performance during the next quarter.

In addition to the tests on the rectifiers, we also performed tests on the clock recovery circuit, the input demodulator, and the local oscillator.

The clock recovery circuit performed as expected. MOS7 uses a high-gain amplifier to recover the clock from the voltage on the micro-coil. The clock recovery performed very well, producing a solid clock signal even for input voltage which were well-below that needed for the rectification.

The input demodulator also performed as expected. Carrier dropouts of as few as one cycle could be detected. This is very encouraging and we will be expanding our testing of the data detection within the next quarter. During that time we will establish the smallest number of carrier cycles which we could use for a state change in the suspended carrier modulation scheme.

The local oscillator exhibited a problem related to bias. Under certain conditions the oscillator would stop and would require a transient to re-start. We have analyzed this problem in simulation and have revised our oscillator circuitry to include a more complicated, but a more robust transconductance amplifier. This new design will be implemented in MOS8. Fortunately we were able to revise MOS7 into MOS8 for submission during this quarter. We expect to receive MOS8 back from MOSIS during the next quarter.

At a much lower level, we have continued to work with the Mann Foundation to quantify the characteristics of the existing AMI 2-MHz microstimulator ASICs so that we may design a suitable 2-MHz transmitter.